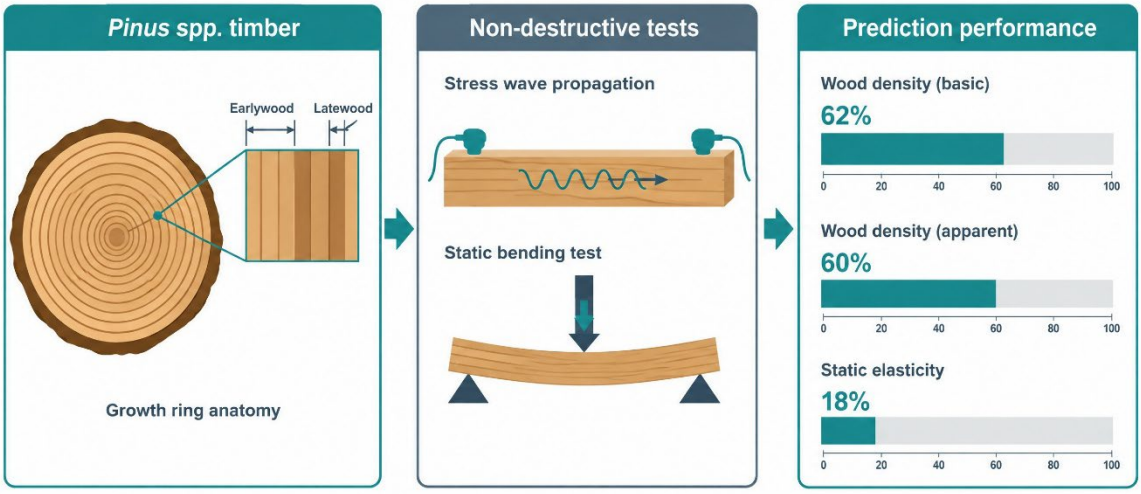
Classification of Tropical *Pinus* spp. Wood Based on Growth Rings

Augusto M. M. Breda [a], Pedro G. A. Segundinho [a,*], Lorenzo L. Santos [b], Leonor C. Mastela [a], Caroline P. Araujo [a], Fabricio G. Gonçalves [a], Juarez B. Paes [a], Clara G. F. Souza [c], Ramon F. Oliveira [a], Vinicius B. Taquetti [a], Yonny M. Lopez [d], Raynord Mayard [a], and Letícia A. A. Ribeiro [a]

* *Corresponding author: p_gutemberg2001@yahoo.com.br*

DOI: 10.15376/biores.21.4.11027-11043

GRAPHICAL ABSTRACT



Classification of Tropical *Pinus* spp. Wood Based on Growth Rings

Augusto M. M. Breda [a], Pedro G. A. Segundinho [a,*], Lorenzo L. Santos [b], Leonor C. Mastela [a], Caroline P. Araujo [a], Fabricio G. Gonçalves [a], Juarez B. Paes [a], Clara G. F. Souza [c], Ramon F. Oliveira [a], Vinicius B. Taquetti [a], Yonny M. Lopez [d], Raynord Mayard [a], and Letícia A. A. Ribeiro [a]

The Brazilian Standard (NBR) for Timber Structures Design must consider, for mechanical grading and structural design, the relationship between the physical–mechanical properties and the growth ring characteristics of *Pinus* spp. Growth ring characteristics are essential variables for estimating the physical–mechanical properties of wood. Therefore, this study aimed to assess the relationship between growth rings and the physical–mechanical properties of defect-free *Pinus* spp. timber. Non-destructive tests were performed, including longitudinal and transverse vibration, stress wave, and static bending tests, as well as the determination of basic and apparent densities, followed by a destructive rupture test. In addition, latewood width, latewood proportion, and the number of growth rings were measured. Pearson's correlation matrix was used to analyze the association between physical–mechanical properties and growth ring characteristics. All Pearson correlation coefficients (r) were significant ($p < 0.05$). The results showed that latewood width explained 62% of basic density and 60% of apparent density, but only 18% of static elasticity. Consequently, the combined assessment of growth ring characteristics and physical–mechanical properties enabled the mechanical characterization of *Pinus* spp. based on growth rings.

DOI: 10.15376/biores.21.4.11027-11043

Keywords: Physical-mechanical properties; Non-destructive testing; Latewood proportion; Static bending testing; Modulus of elasticity

*Contact information: a: Department of Forest and Wood Science, Federal University of Espírito Santo, Avenida Governador Lindemberg, Jerônimo Monteiro 29550-000, ES, Brazil; b: Foundation for Assistance and Education – FAESA, University Center, Av. Vitória, Monte Belo, Vitória 29053-360, ES, Brazil; c: São Carlos School of Engineering, University of São Paulo, Avenida Trabalhador São Carlense, 400, Parque Arnold Schimidt, São Carlos 13566-590, SP, Brazil; d: São Félix do Xingu Campus, Federal University of South and Southeast Pará, Avenida Norte Sul, Loteamento Cidade Nova, São Felix do Xingu 68380-000, PA, Brazil; * Corresponding author: p_gutemberg2001@yahoo.com.br*

INTRODUCTION

In 2024, the planted forest sector in Brazil reached a total of 10.52 million hectares, of which 1.9 million hectares are allocated to *Pinus* spp. plantations, whose wood has wide industrial applicability in the production of sawn timber, panels, pulp, and paper (IBÁ 2025; Mensah *et al*. 2025). For centuries, conifer stakes have been used in the construction of city foundations, demonstrating their ability to withstand structural loads (Pagella *et al*. 2024). In addition to their economic importance, these forests also provide essential ecosystem services, mainly through the sequestration of carbon from the atmosphere (IBÁ 2025).

Pinus wood, classified as softwood (conifers), differs from hardwoods (broadleaves) in several anatomical aspects, directly influencing its technological properties. Among the anatomical elements of wood, growth rings stand out and are considered reliable indicators of its physical-mechanical properties, especially those intended for structural use. They are formed from the activity of the vascular cambium and are divided into earlywood and latewood, generally being visible and well defined in conifers (Ruffinatto *et al*. 2023). This characteristic is observed for *P. elliottii* in tropical regions of South America, in addition to its rapid growth and resistance to climatic variations (Olmedo *et al*. 2023). In tropical regions, different environmental factors can impact tree growth, including temperature, precipitation, soil moisture, and periods of flooding and drought. These factors affect cambial activity and influence the formation of tree growth rings (Pumijumnong *et al*. 2023).

The variation in the width of the growth rings and in the proportion between earlywood and latewood affects essential attributes for structural performance, such as basic density and shrinkage (Stöd *et al*. 2025). In this context, the proportion of latewood in the growth rings can influence the mechanical strength of *Pinus* sp. wood, since this tissue generally presents a higher modulus of rupture compared to earlywood and the transition zone (Konukcu *et al*. 2021). Latewood also has a greater deflection capacity (deformation before rupture) (Mańkowski *et al*. 2025) and higher density (Konukcu *et al*. 2021) compared to earlywood. Characteristics such as apparent density, radial shrinkage, and tensile strength are also positively correlated with the percentage of latewood present in the wood (Wang *et al*. 2022).

The tracheids that compose the growth rings tend to present larger diameters at the base of the trunk, decreasing toward the apex. This anatomical variation is directly reflected in the basic density, modulus of elasticity, and modulus of rupture of the wood, which generally present higher values near the base and lower values toward the apex (Górska *et al*. 2025). In conifers, the width of the growth rings also influences these characteristics (Wang *et al*. 2022). In addition, the mechanical strength of wood varies according to the orientation of the fibers (longitudinal, radial, and tangential), due to its orthotropic nature (Konukcu *et al*. 2021).

The structural classification of wood is fundamental for estimating its strength and potential for use, ensuring safety in structural applications. Therefore, this study investigated possible improvements in the mechanical classification of *Pinus* spp. wood based on the relationship between growth rings, latewood, and static bending, according to Part 2: Test Methods for Visual and Mechanical Classification of Structural Timber Pieces of the Brazilian Standard—NBR 7190-2, of the Brazilian Association of Technical Standards ABNT) (NBR 7190-2 2022). This perspective is aligned with current discussions on the revision of the standard, since, according to Lahr *et al*. (2022), it underestimates wooden structures by considering that they support lower loads than they can actually withstand.

The originality of this study involves a broad data sampling, integrating anatomical characteristics of growth rings and physical-mechanical properties of *Pinus* spp. wood through destructive and non-destructive testing. This information contributes to strengthening the structural grading of *Pinus* spp. wood, in order to complement the NBR 7190-2 standard. In view of this, the objective of this study is to evaluate the relationship between growth rings and the physical-mechanical properties of *Pinus* spp. wood, subjected to destructive and non-destructive tests, aiming to generate information that contributes to mechanical grading for structural applications.

EXPERIMENTAL

Species, Wood Origin and Tests Performed

For this study, *Pinus* spp. wood obtained from the material used by Santos (2019) was employed, which was supplied by Berneck S.A. Painéis e Serrados. A total of 1,500 boards measuring 38 × 89 × 3,960 mm, with a moisture content of 12%, were provided. The batch consisted of a mixture of *Pinus taeda* and *Pinus elliottii* wood, grown and processed in the Curitibanos region, Santa Catarina, Brazil. In total, 426 *Pinus* spp. specimens were tested and divided into groups according to their grain orientation (tangential, radial, and radial–tangential).

The tests for determining physical–mechanical properties and visual characteristics were carried out at the Wood Structures Laboratory, Department of Forest and Wood Sciences, Center for Agricultural Sciences and Engineering, Federal University of Espírito Santo, following the specifications of NBR 7190-2 (2022) and, in specific cases, ISO 13910 (2005) and ASTM D-143 (2022).

The specimens used in the bending tests were also employed to determine basic and apparent densities, and latewood width and proportion. The specimens were measured in the longitudinal, radial, and tangential directions using a ruler (graduated in mm) to measure length, and a digital caliper (0.005 mm precision) to obtain width and thickness. After measuring, they were weighed with a precision balance (0.01 g precision) to determine apparent density. The spans for the supports of each test were then marked according to the requirements of NBR 7190-2 (2022) and ASTM D-143 (2022), in accordance with the experimental test to be performed.

The growth rings were counted visually, and the wood was classified, based on the proportion of latewood, as dense (> 1/2) or light (< 1/2), according to density classes adapted from ASTM D245-22 (2022). This procedure was necessary because the specimens analyzed in the ImageJ software, measured approximately 2 × 2 × 3 cm^3 (width × thickness × length). These specimens were used for basic density analysis and counting the number of annual rings (NAC). The NAC corresponds to the number of growth rings present in the samples analyzed for each treatment, with the images aligned perpendicular to the growth rings.

Tests

Free transverse and longitudinal vibration tests

The timber specimens (49.88 cm × 3.8 cm × 2.26 cm) were tested under free transverse and longitudinal vibration to determine the dynamic modulus of elasticity, using Sonelastic® software, version 6.0 (ATCP Engenharia Física, Ribeirão Preto, SP, Brazil), a computer, a microphone, and a specific hammer to excite the samples.

The free transverse vibration test was conducted in accordance with ASTM E1876-22 (2022) and ASTM C215-20 (2020). The longitudinal vibration test was performed according to ASTM E1876-22 (2022) and as described by Segundinho *et al*. (2018).

After markings were made on the specimens, they were placed on supports consisting of two Nylon® lines. A microphone was positioned beneath the specimen, directly below the marking at the center of the piece and was connected to a computer equipped with a data acquisition system. On the upper side, at the center marking, an impact was applied using a hammer. The vibration generated by the impact and propagated along the specimen was captured by the microphone.

Stress wave test

Two dynamic moduli of elasticity were obtained using stress waves. Tests were performed using two different stress wave timer devices (Fakopp Kft., Sopron, Hungary and Metriguard Inc. model 239A, Pullman, WA, USA). The stress wave tests with the Fakopp device followed the procedures described by Paula *et al*. (2016).

The specimens used in the free transverse vibration and longitudinal vibration tests (49.88 cm × 3.8 cm × 2.26 cm) were also employed in the stress wave tests. They were positioned between two accelerometers installed at their ends, whose function was to emit and receive the stress wave. A hammer specifically designed for the Fakopp Stress Wave Timer equipment was used to generate the impact on the starting accelerometer. Upon impact, the wave propagated through the specimen until reaching the receiving accelerometer. Three measurements of the wave propagation time were performed. Using propagation time data, the dynamic modulus of elasticity (E_{ds}) in the longitudinal direction of the specimen was calculated. The same equation used to calculate E_{ds} with the Fakopp device (Cunha 2010) was also applied to determine the dynamic modulus of elasticity using the Metriguard stress wave timer.

For the Metriguard stress wave timer, the protocol described by Gonçalez *et al*. (2018) was followed. Three readings of the propagation time were taken, and the mean value of these three readings was used to calculate the dynamic modulus of elasticity. Thus, the E_{ds} was obtained.

Static bending and rupture tests

The static bending test was conducted according to Candaten *et al*. (2018) using an EMIC universal testing machine (10 kN capacity) (EMIC, São José dos Pinhais, PR, Brazil), equipped with an automated data acquisition system, following ASTM D-143 (2022). The evaluated variables were the static modulus of elasticity (E_M) and the modulus of rupture (R_p), determined using specimens with dimensions of 49.88 cm × 3.8 cm × 2.26 cm. The equipment includes a reaction frame, an electromechanical testing machine, and bending fixtures that allow measurement of vertical load displacements.

To determine the modulus of rupture (R_p), the test followed the same methodology used for determining the static modulus of elasticity. However, the system was calibrated to cause the structural specimen to fail. The values obtained by the universal testing machine in the rupture test, expressed in kgf·cm^{-2}, were converted to MPa. The span is equal to 47.46 mm.

Latewood width and proportion

Among the growth ring characteristics, latewood proportion (PLT, in %) and latewood width (LWT, in mm) were evaluated using specimens with dimensions of 2 × 2 × 3 cm^3. To determine PLT and LWT, the specimens were scanned using an Epson Perfection V750 scanner (Seiko Epson Corporation, Nagano, Japan). The images were then analyzed with the open-source software ImageJ® version 1.49 (Schneider *et al*. 2012), after conversion to 8-bit resolution (black and white). Before analysis, the software was calibrated.

Data analysis

The R software, version 4.2.1 (R Core Team 2021), was used as the computational–statistical tool for descriptive statistical analyses. The following statistical measures were

calculated: mean, median, maximum and minimum observed values, and sample standard deviation.

The specimens were divided into groups according to their orientations: tangential, radial, and radial–tangential. A completely randomized design (CRD) was adopted. The tangential, radial, and radial–tangential treatments were subjected to Analysis of Variance (ANOVA) followed by Tukey's test ($p < 0.05$). The treatments had different numbers of replications: tangential: six replications; radial: 121 replications; radial–tangential: 299 replications. The mean values of each treatment—that is, the means of all variables (moduli of elasticity and rupture, basic and apparent densities, latewood proportion, latewood width and number of growth rings)—were evaluated using Tukey's test ($p < 0.05$). Next, the physical–mechanical properties of the wood and the growth ring characteristics were subjected to the Anderson–Darling normality test ($p < 0.05$). After confirming that the data did not follow a normal distribution, nonparametric statistical analysis was conducted. The χ^2 (chi-square) test ($p < 0.05$) was applied to verify independence among the variables. Once independence was established, the Kruskal–Wallis test ($p < 0.05$) was used to compare medians, which is appropriate for non-normally distributed data.

Finally, the correlation among all physical–mechanical properties of the wood and the growth ring characteristics was assessed using the Pearson correlation matrix ($p < 0.05$). To construct the matrix, the Pearson correlation coefficient (r) was calculated for each pair of variables (x and y) included in this study. The mean of each variable ($\bar{x}$ and $\bar{y}$) was computed, and the r coefficient was obtained following (Montgomery and Runger 2016). The value of r indicated the strength of the relationship between variables, demonstrating the percentage of variation in one variable explained by the other. The Pearson correlation matrix was generated using the statistical software R Core Team (2021).

RESULTS AND DISCUSSION

Growth Ring Characteristics and Physical–Mechanical Properties of *Pinus* spp. Wood

Table 1 presents the mean values of the growth ring characteristics of *Pinus* spp. wood for the tangential, radial, and radial–tangential orientations.

Table 1. Growth Ring Characteristics of *Pinus* spp. Wood for the Tangential, Radial, and Radial–Tangential Orientations

Orientation	Variables		
	PLT (%)	LWT (mm)	NAC
Tangential	16.91 b (23.42)	5.92 c (25.34)	2.67 b (30.34)
Radial	23.38 a (31.91)	9.11 b (40.83)	4.20 a (38.57)
Radial-Tangential	22.89 a (32.15)	11.12 a (35.34)	4.49 a (41.87)

In parentheses: Relative Standard Deviation (RSD%); PLT: latewood proportion; LWT: latewood width; NAC: number of annual rings. Means followed by the same letter do not differ statistically from one another (Tukey, $p \geqslant 0.05$).

The mean values for the tangential orientation differed from the others in latewood proportion and number of annual rings, while all means differed for variable latewood proportion. One possible explanation for these differences is the characteristics of the specimens in each orientation. Table 2 shows the mean basic and apparent densities of *Pinus* spp. wood.

Table 2. Apparent and Basic Densities of *Pinus* spp. Wood for the Tangential, Radial, and Radial–Tangential Orientations

Orientation	Variables	
	ρ_{ap} (g·cm^{-3})	ρ_{bas} (g·cm^{-3})
Tangential	0.41 b (7.32)	0.34 b (8.82)
Radial	0.45 a (11.11)	0.37 a (13.51)
Radial-Tangential	0.44 a (13.64)	0.37 a (13.51)

In parentheses: Relative Standard Deviation (RSD%); ρ_{ap}: apparent density; ρ_{bas}: basic density. Means followed by the same letter do not differ statistically from one another (Tukey, $p \geqslant 0.05$).

The ρ_{ap} values were similar in the radial and radial–tangential directions and were higher compared to the tangential direction. Melo *et al*. (2013) concluded that the density of *P. elliottii* wood is affected by sample orientation, varying from the base to the top (longitudinal direction) and from pith to bark (axial direction). Table 3 presents the physical–mechanical properties of *Pinus* spp. wood.

Table 3. Physical–Mechanical Properties of *Pinus* spp. Wood for the Tangential, Radial, and Radial–Tangential Orientations

Orientation	Variables					
	E_{al} (GPa)	E_{vt} (GPa)	$E_{ds(F)}$ (GPa)	$E_{ds(M)}$ (GPa)	E_M (GPa)	R_p (MPa)
Tangential	8.94 a (18.79)	8.79 a (21.16)	8.56 a (13.54)	7.99 a (17.27)	6.97 a (7.75)	63.88 a (19.83)
Radial	8.73 a (30.47)	8.22 a (30.41)	8.60 a (25.47)	8.05 a (27.08)	6.49 b (17.57)	66.84 a (23.80)
Radial-Tangential	9.10 a (33.63)	8.59 a (33.18)	8.80 a (28.52)	8.21 a (30.09)	6.52 b (20.71)	66.56 a (25.08)

In parentheses: Relative Standard Deviation (RSD%); E_{al}: dynamic modulus of elasticity obtained through the longitudinal vibration method; E_{vt}: dynamic modulus of elasticity obtained through the free transverse vibration method; $E_{ds(F)}$: dynamic modulus of elasticity from stress-wave timing obtained using the Fakopp device; $E_{ds(M)}$: dynamic modulus of elasticity from stress-wave timing obtained using the Metriguard device; E_M: static modulus of elasticity; R_p: modulus of rupture. Means followed by the same letter do not differ statistically (Tukey, $p \geqslant 0.05$).

In general, the dynamic moduli of elasticity E_{al}, $E_{ds(F)}$, and $E_{ds(M)}$, as well as LWT and NAC, were higher in the radial–tangential direction, whereas E_{vt} and E_M were higher in the tangential direction, and R_p, PLT, and ρ_{ap} were higher in the radial direction. Basic density did not differ between the radial and radial–tangential directions. Table 4 presents the general descriptive statistics for all variables.

Table 4. Descriptive Statistics of Growth-Ring Characteristics, Apparent and Basic Densities, and Mechanical Properties of *Pinus* spp.

Variables	Descriptive Statistics				
	Minimum	Median	Mean	Maximum	RSD
E_{al} (GPa)	3.13	8.67	8.99	22.40	32.70
E_{vt} (GPa)	2.65	8.21	8.49	21.16	32.27
$E_{ds(F)}$ (GPa)	3.47	8.59	8.74	19.52	27.57
$E_{ds(M)}$ (GPa)	3.20	7.97	8.16	18.94	29.17
E_M (GPa)	2.44	6.92	6.52	9.52	19.79
R_p (MPa)	25.02	64.99	66.60	132.63	24.61
ρ_{ap} (g·cm^{-3})	0.32	0.44	0.45	0.69	13.33
ρ_{bas} (g·cm^{-3})	0.26	0.37	0.37	0.61	13.51
PLT (%)	6.22	22.26	22.95	49.88	32.16
LWT (mm)	1.52	9.88	10.47	29.29	38.01
NAC (unit)	1.00	4.00	4.38	14.00	41.32

RSD: Relative Standard Deviation (%); E_{al}: dynamic modulus of elasticity obtained via longitudinal vibration; E_{vt}: dynamic modulus of elasticity obtained via free transverse vibration; $E_{ds(F)}$: dynamic modulus of elasticity from stress-wave timing using the Fakopp device; $E_{ds(M)}$: dynamic modulus of elasticity from stress-wave timing using the Metriguard device; E_M: static modulus of elasticity; R_p: modulus of rupture; ρ_{ap}: apparent density; ρ_{bas}: basic density; PLT: proportion of latewood; LWT: latewood width; NAC: number of growth rings.

The maximum latewood proportion was 49.88%. Therefore, no dense specimens were identified in this experiment, which requires values greater than half of the total area displayed by the software for a specimen to be classified as dense. This also prevented dividing the groups into dense and non-dense within the tangential, radial, and radial–tangential orientations.

Apparent and Basic Densities

For apparent density (ρ_{ap}), Ballarin and Palma (2003) classified wood as mature and juvenile wood, with mean values above the significance level adopted in this study. Almeida *et al*. (2014) reported an average apparent density of 0.50 g·cm^{-3} for *Pinus* sp. wood, which is higher than that obtained in the present work.

For *Pinus* sp. wood, Segundinho *et al*. (2017) found a value of 0.56 g·cm^{-3}, also higher than the ρ_{ap} value reported here. Mustefaga *et al*. (2019) found apparent density values of 0.32 and 0.41 g·cm^{-3} for *Pinus patula* and *Pinus taeda*, respectively, which are lower than those found in this study and were considered low by the authors.

In Ferreira *et al*. (2023), the following apparent density values for *P. elliottii* at different moisture contents were reported: 0.82 g·cm^{-3} (90% moisture), 0.695 g·cm^{-3} (60% moisture), 0.591 g·cm^{-3} (30% moisture), 0.564 g·cm^{-3} (25% moisture), 0.556 g·cm^{-3} (20% moisture), 0.540 g·cm^{-3} (15% moisture), 0.531 g·cm^{-3} (12% moisture), 0.526 g·cm^{-3} (11% moisture), 0.509 g·cm^{-3} (5% moisture) and 0.484 g·cm^{-3} (0% moisture). All values are higher than the 0.45 g·cm^{-3} apparent density (at the reference moisture content of 12% for the manufactured specimens) found in the present study. According to the authors, among the forest species evaluated (*P. elliottii* and *Bertholletia excelsa*), wood with lower density values (ρ_{ap} and ρ_b) showed greater variation in mechanical properties and a lower static modulus of elasticity than wood with generally higher density.

Gonçalez *et al*. (2018) studied the relationship between growth rings and mechanical properties in *Pinus caribaea*, obtaining basic densities of 0.51 g·cm^{-3} for samples with growth-ring widths between 0 and 0.7 mm, 0.46 g·cm^{-3} for widths between

0.7 and 1.2 mm, and 0.41 g·cm^{-3} for widths between 1.2 and 2 mm. They concluded that the narrower growth rings combined with a higher proportion latewood result in greater basic density.

Dynamic Moduli of Elasticity

For the relationship between growth rings and mechanical properties in *P. caribaea* samples with different ring widths, Gonçalez *et al*. (2018) found $E_{ds(M)}$ values of 17.7 GPa for ring widths between 0 and 0.7 mm; 12.6 GPa for ring widths between 0.7 and 1.2 mm; and 10.4 GPa for ring widths between 1.2 and 2 mm. Notably, as growth-ring width increases and latewood proportion decreases, the dynamic modulus of elasticity also decreases. These values are still above the mean $E_{ds(M)}$ of 8.16 GPa obtained in this study, although they are lower than the maximum $E_{ds(M)}$ value of 18.94 GPa.

Erasmus *et al*. (2018), studying the effect of different spacings on microfibril angle and density in *P. patula*, obtained $E_{ds(F)}$ values ranging from 10.2 to 15.0 GPa. These values are higher than the mean of 8.74 GPa and lower than the maximum of 19.52 GPa found in this research.

Another method for determining the dynamic modulus of elasticity is transverse vibration testing. Segundinho *et al*. (2017), evaluating the influence of moisture content on the elastic modulus of *Pinus* sp., obtained maximum E_{vt} values around 14 GPa for moisture contents below 20%, which is lower than the maximum E_{vt} value of 21.2 GPa found in the present study. Ferreira *et al*. (2023), analyzing the relationship between moisture, density, and wave propagation in *Pinus* sp., found E_{vt} values that varied with moisture content, with the highest value in transverse vibration being 11.5 GPa at 5% moisture—higher than the mean of 8.49 GPa found in this work.

On average, the maximum values of the dynamic modulus of elasticity obtained *via* longitudinal vibration in this study were higher than those obtained by other dynamic methods, particularly transverse vibration. This is because most samples in this research had a higher proportion of latewood and smaller latewood width, in addition to being free of defects, which improved the maximum values obtained through longitudinal vibration testing.

Although the minimum E_{al} value obtained in this work was lower than the dynamic moduli obtained by stress-wave methods $E_{ds(M)}$ and $E_{ds(F)}$, the longitudinal vibration test proved to be the most suitable method for determining the dynamic modulus of elasticity and for the mechanical characterization of the wood. This is because knowledge of the dynamic modulus of elasticity allows for better allocation of structural members according to wood strength (Andrade Junior 2016).

Static Modulus of Elasticity

NBR 7190-2 (2022) defines tension and compression as the mechanical properties used for structural classification, evaluated in two directions (parallel and perpendicular to the grain). However, static bending is a property from which two essential parameters for structural design can be obtained (the static modulus of elasticity and the modulus of rupture). Therefore, for a proposed mechanical classification of defect-free *Pinus* sp. wood, this property must be examined.

Ballarin and Palma (2003), studying for the strength and stiffness of *Pinus* sp., found an average value of 16.7 GPa for the *E* in mature *P. taeda* wood. This value is higher than the mean found in the present study, 6.52 GPa. As the authors highlight, mature wood performs better than juvenile wood regarding the elastic modulus in static bending.

Regarding stand spacing, Hébert *et al*. (2016), studying *Pinus banksiana*, concluded that spacing itself did not affect the *E*; instead, performance differed between juvenile and mature samples. Trianoski *et al*. (2014), investigating the mechanical properties of tropical *Pinus* species, found static *E* values ranging from 6.06 to 8.94 GPa, which are below and above, respectively, the mean of 6.52 GPa found in this study. The authors reported that *P. maximinoi*, *P. tecunumanii* and *P. oocarpa* showed the best strength and stiffness performance.

With respect to moisture content effects on the elastic modulus of *Pinus* sp., Segundinho *et al*. (2017) obtained a maximum *E* of approximately 14 GPa for moisture contents below 20%. Essien *et al*. (2017) reported a mean value of 7.97 GPa for *P. taeda*.

In an experiment with *Pinus caribaea*, Gonçalez *et al*. (2018) examined the relationship between growth ring width and static bending *E*, obtaining mean values of 8.67 GPa for ring width between 0 and 0.7 mm, 10.05 GPa for 0.7 to 1.2 mm, and 11.57 GPa for 1.2 to 2 mm. Mustefaga *et al*. (2019), investigating juvenile wood of *Pinus* sp., obtained *E* values of 6.32 GPa for *P. patula* and 6.63 GPa for *P. taeda*. This difference is attributed to the fact that the growth rings in the samples of this study (although defect-free) contained a higher proportion of latewood width than those in Gonçalez *et al*. (2018), resulting in lower static elasticity values in this study.

Modulus of Rupture

Regarding *R*, Ballarin and Palma (2003) found an average value of 127.6 MPa in mature *P. taeda* wood. Hébert *et al*. (2016) concluded that tree spacing did not affect *R*, although sampling influenced *R* values. Essien *et al*. (2017) reported an average *R* value of 74.5 MPa for *P. taeda*.

In comparison, Gonçalez *et al*. (2018), for ring width intervals of 0 to 0.7 mm, 0.7 to 1.2 mm and 1.2 to 2 mm, found *R* values of 93.5 MPa, 101.7 MPa and 80.2 MPa, respectively. Additionally, Mustefaga *et al*. (2019), reported mean *R* values of 45.3 MPa for juvenile *P. patula* wood and 56.3 MPa for juvenile *P. taeda* wood.

Growth rings influence mechanical strength, as assessed by the modulus of rupture, through density: a higher proportion of latewood and smaller latewood width result in higher density and greater mechanical strength (Rall 2006). When specimens are free of defects, the *R* reflects higher mechanical strength, because defects hinder accurate determination of the physical–mechanical properties of *Pinus* sp. wood (Calil Junior 2003).

Number of Growth Rings, Latewood Width and Latewood Proportion

In Wood Science and Technology, the variables number of growth rings, latewood width, and latewood proportion are part of tree growth analysis. All these properties share a functional relationship, as they are defined based on growth rings. Growth rings are correlated with other variables, such as physical properties (basic and apparent density) and mechanical properties (modulus of elasticity and modulus of rupture).

Regarding latewood width (LWT), dendrochronological evidence presented by Arzac *et al*. (2018), studying *Pinus sylvestris*, revealed that annual ring-width increment may predict, through modeling, potential variations in mechanical properties driven by climate change. In their study, increased tracheid thickness during rainy periods enhanced anatomical structural properties and, consequently, the physical–mechanical properties and ring characteristics. Gonçalez *et al*. (2018), for *Pinus caribaea*, concluded that the narrower the growth rings and the higher the presence of latewood, the greater the basic density.

Furthermore, the authors emphasized that both the modulus of elasticity and the modulus of rupture are higher in woods with narrower growth rings, that is, with smaller ring width.

For three classes of 60-year-old *P. sylvestris* L., Fabisiak and Fabisiak (2021) reported annual LWT variance values of 3.44 mm for the dominant class, 2.39 mm for the intermediate class and 1.54 mm for the suppressed class. The narrowest growth rings were found in the suppressed class, which had the lowest LWT values. Thus, the suppressed class would be most suitable for structural design, where density and ring characteristics are crucial. Fabisiak and Fabisiak (2021) also reported that the suppressed class had the highest latewood proportion and density. However, all values obtained by these authors were lower than those found in the present study, which had an average LWT of 10.47 mm.

Environmental and climate conditions also influence LWT, as demonstrated in *Pinus kesiya* ring-parameter chronologies studied by Thomte *et al*. (2022). Among the parameters assessed was latewood width. The authors observed that earlywood represented most of the ring over time, while latewood occupied a smaller area. This observation aligns with the LWT analyses in the present study, where latewood proportion did not exceed 50% of the total ring area analyzed in ImageJ.

Regarding latewood proportion (LWP), Topanotti *et al*. (2021) observed that both latewood width and latewood proportion affected ring density in *P. taeda*, with LWP having the greatest influence. The authors also noted that LWP increases with age, contributing to increased tree density and indicating whether the wood is juvenile or mature. For classification purposes, LWP should reach or exceed 50%, which did not occur in their experiment and corroborates the results of this study, whose maximum latewood proportion was 49.9%.

Adamopoulos *et al*. (2009), studying latewood width and proportion in *Pinus brutia* from reforestation areas in northern Greece, reported mean LWT values of 4.9 mm across three stem heights (base, mid-height and upper stem) in high-quality soils (deeper soils with greater water availability) and 4.3 mm in medium-quality soils. For LWP, mean values were 16.5% in high-quality soils and 15.6% in medium-quality soils. Both the LWT and LWP values found in that study were lower than those observed in the present work (mean LWP of 23.0% and mean LWT of 10.5 mm).

Dias *et al*. (2018), investigating intra- and inter-tree variation in *Pinus nigra* density across different sites in Portugal, found an overall mean LWP of 38.9%, higher than the mean in the present study. For LWT, the authors reported an overall mean of 0.87 mm per ring and concluded that planting site significantly influenced LWP.

Correlation Analysis Between Growth Ring Characteristics and the Physical–Mechanical Properties of *Pinus* spp. Wood

Table 5 presents the Anderson–Darling (AD) test values for data normality. It was verified that the data did not follow a normal distribution. Therefore, the statistical analysis used in this study was non-parametric. The null hypothesis was rejected, and the independence of the variables was subsequently evaluated. This step is necessary for selecting the appropriate test for comparing means. In this study, the Kruskal–Wallis test was used to determine whether the samples in which independence between two means was verified originated from populations with the same means. To verify the independence between two means, the χ^2 test was applied. Based on the analysis of the χ^2 results, the test indicated an association between the following pairs of variables: E_{al} and E_{vt}; E_{al} and R_p; E_{al} and NAC; E_{vt} and R_p; E_{vt} and NAC; and R_p and NAC. Therefore, these variable combinations were not selected for the Kruskal–Wallis ($p < 0.05$) median comparison test,

since one of the assumptions of this test—used to compare samples from two populations with the same means—is that the samples must be independent.

Table 5. Anderson–Darling Test for Data Normality

Variables	AD	*p*-Value
E_{al}	3.25	3.60×10^{-8}
E_{vt}	3.00	1.47×10^{-7}
$E_{ds(F)}$	2.76	5.86×10^{-7}
$E_{ds(M)}$	2.32	6.93×10^{-6}
E_M	15.30	2.20×10^{-16}
R_p	4.18	2.08×10^{-10}
ρ_{ap}	4.05	4.31×10^{-10}
ρ_{bas}	4.99	2.33×10^{-12}
PLT	1.46	8.88×10^{-4}
LWT	2.77	5.36×10^{-7}
NAC	16.88	2.2×10^{-16}

AD: Anderson–Darling test statistic.

The Kruskal–Wallis test shows that the medians of the static modulus of elasticity, compared with the medians of the dynamic moduli of elasticity obtained by longitudinal and transverse vibration, are significantly different. Similarly, the medians of the dynamic modulus of elasticity obtained by stress waves, compared with the medians of the dynamic moduli obtained by longitudinal and transverse vibration, also differ according to the Kruskal–Wallis test. To construct the Pearson correlation matrix, the Pearson correlation coefficient (r) was calculated for each pair of variables. The significance of the Pearson r coefficients was then tested ($p < 0.05$).

Table 6 presents the Pearson correlation matrix for the data obtained in this study. The matrix was used as a statistical tool to analyze the correlations between the physical–mechanical properties and the growth ring characteristics.

Table 6. Pearson Correlation between the Physical–Mechanical Properties and Growth Ring Characteristics of *Pinus* spp.

	E_{al}	E_{vt}	$E_{ds(F)}$	$E_{ds(M)}$	E_M	R_p	ρ_{ap}	ρ_{bas}	PLT	LWT	NAC
E_{al}	1.00										
E_{vt}	0.99	1.00									
$E_{ds(F)}$	0.98	0.97	1.00								
$E_{ds(M)}$	0.96	0.95	0.97	1.00							
E_M	0.80	0.80	0.80	0.77	1.00						
R_p	0.78	0.78	0.78	0.75	0.60	1.00					
ρ_{ap}	0.64	0.63	0.67	0.64	0.39	0.79	1.00				
ρ_{bas}	0.49	0.48	0.51	0.49	0.27	0.67	0.85	1.00			
PLT	0.39	0.37	0.40	0.38	0.20	0.53	0.70	0.66	1.00		
LWT	0.35	0.33	0.36	0.34	0.18	0.47	0.60	0.62	0.76	1.00	
NAC	0.65	0.64	0.66	0.64	0.45	0.60	0.56	0.52	0.57	0.56	1.00

E_{al} (GPa): Dynamic modulus of elasticity obtained by the longitudinal vibration method; E_{vt} (GPa): Dynamic modulus of elasticity obtained by the free transverse vibration method; $E_{ds(F)}$ (GPa): Dynamic modulus of elasticity by stress wave obtained with the Fakopp equipment; $E_{ds(M)}$ (GPa): Dynamic modulus of elasticity by stress wave obtained with the Metriguard equipment; E_M (GPa): Static modulus of elasticity; R_p (MPa): Modulus of rupture; ρ_{ap} ($kg \cdot m^{-3}$): Apparent density; ρ_{bas} ($g \cdot cm^{-3}$): Basic density; PLT (%): Latewood proportion; LWT (mm): Latewood width; NAC: Number of growth rings. Correlation values are significant ($p < 0.05$)

All correlations were significant ($p < 0.05$). Pearson correlation coefficients ranged from 0.18 for the correlation between E_M and LWT to 0.99 for the correlation between E_{al} and E_{vt}. The high correlation between the dynamic moduli of elasticity obtained from the longitudinal and transverse vibration tests corroborates the χ^2 test for variable independence, which indicated that these variables are dependent on each other. The lowest values were found for the correlation between the static modulus of elasticity and latewood width, where latewood width explained 18% of E_M, latewood proportion explained 20% of E_M, and basic density explained 27% of the static modulus of elasticity.

Ballarin and Palma (2003) reported a significant correlation between the moduli related to static bending (E_M and R) in mature wood of *P. taeda*. Essien *et al*. (2017) found a high correlation of 0.92 between E_M and R_p, higher than the value obtained in this study. Erasmus *et al*. (2018) observed a negative correlation between LWT and PLT and between LWT and density, differing from the findings of this research, although significant within their study.

Using a stress wave timer, Gonçalez *et al*. (2018) determined that better correlations were obtained than with ultrasound. That study reported high correlation values for different growth ring width intervals within the range of 0 to 0.7 mm: a correlation of 0.593 between E_M and E_{ds}, and 0.614 between R and E_{ds}. Both results were lower than the correlations found in this research. Only the correlation between E_M and R_p performed better in the growth ring width interval of 1.2 to 2 mm, reaching 0.926—higher than the value found in this study.

Mustefaga *et al*. (2019) demonstrated a strong correlation between apparent density and most mechanical properties, clearly indicating that apparent density can be used to estimate strength and stiffness parameters. Therefore, considering the physical properties (basic and apparent densities) and the fact that the specimens were free of defects, it may be affirmed, in line with Santos (2019), that density values are among the causes of variation in the results of the other variables analyzed in this study.

In this context, the correlations obtained in this study represent degrees of association between variables in small, clear specimens. However, for timber structural design, Zangiacomo, Christoforo and Rocco Lah (2013) argue that such inference, derived from small specimens, may lead to less safe structural designs compared with those carried out using full-size structural members. A similar viewpoint is found in Moritani and Calil Junior (2019); even in defect-free small specimens, it is not possible to ascertain the best parameters for members of structural dimensions.

Although compression and tension are the most suitable methods to estimate the modulus of elasticity for structural timber elements, static bending and rupture tests may also be used in the mechanical grading of *Pinus* spp. timber, provided that the tests are conducted on structural-size members.

CONCLUSIONS

1. Given the characteristics of the analyzed material, all timber specimens were classified as non-dense, which prevented a comparison between dense and non-dense groups.
2. Latewood width (LWT) showed a moderate correlation with density properties (ρ_{bas} = 0.62; ρ_{ap} = 0.60) and a weak correlation with E_M (0.18), evidencing a greater influence on wood density and a low influence on its stiffness.

3. Anatomical orientations influenced the density properties of ρ_{bas} and ρ_{ap} of the wood, with higher values in the radial and radial–tangential orientations, demonstrating that it is a relevant factor related to the physical properties of wood.
4. The dynamic modulus of elasticity (E_{al}, E_{vt}, $E_{ds(F)}$ and $E_{ds(M)}$) showed high correlations with E_M, ranging from 0.77 to 0.80, demonstrating the efficiency of non-destructive methods in evaluating wood stiffness. There was also a high correlation between non-destructive methods, with r ranging from 0.95 to 0.99, indicating reliability in the characterization of the studied material by the different methods.
5. The results obtained in this study complement NBR 7190-2, acting as additional support for the characterization of *Pinus* spp. wood, without replacing the established normative tests.

ACKNOWLEDGMENTS

This research was funded by the "Fundação de Amparo à Pesquisa e Inovação do Estado do Espírito Santo" (FAPES/SEAG notice No 06/2015—PPE AGROPECUÁRIA), grant number (T.O. No 720/2016), and by the "Conselho Nacional de Desenvolvimento Cientifico e Tecnológico (CNPq)", process number 409045/2016-0, with Professor Dr. Pedro Gutemberg de Alcântara Segundinho as the applicant, Call: Universal 2016, referring to the project "Avaliação numérica e experimental de vigas madeira laminada colada (MLC) produzidas de Eucalipto".

Conflict of Interest

The authors declare that there are no conflicts of interest.

Use of Generative AI

The authors declare that they did not use AI tools in the preparation of this manuscript.

REFERENCES CITED

Adamopoulos, S., Milios, E., Doganos, D., and Bistinas, I. (2009). "Ring width, latewood proportion and dry density in stems of *Pinus brutia* Ten.," *Eur. J. Wood Wood Prod.* 67, 471-477. https://doi.org/10.1007/s00107-009-0345-x

Almeida, D. H. D., Scaliante, R. M., Christoforo, A. L., Varanda, L. D., Lahr, F. A. R., Dias, A. A., and Calil Junior, C. (2014). "Tenacidade da madeira como função da densidade aparente," *Rev. Árvore* 38(1), 203-207. https://doi.org/10.1590/S0100-67622014000100020

Andrade Junior, J. R. (2016). *Classificação Estrutural de Peças de Madeira de Pinus elliottii Utilizando o Módulo de Elasticidade Obtido Pelo Método de Ondas Longitudinais de Tensão*, Master's Thesis, Universidade de São Paulo, São Carlos, Brazil.

Arzac, A., Babushkina, E. A., Fonti, P., Slobodchikova, V., Sviderskaya, I. V., and Vaganov, E. A. (2018). "Evidences of wider latewood in *Pinus sylvestris* from a forest-steppe of Southern Siberia," *Dendrochronologia* 49, 1-8.

https://doi.org/10.1016/j.dendro.2018.02.007
ASTM C215-20 (2020). "Standard test method for fundamental transverse, longitudinal, and torsional resonant frequencies of concrete specimens," ASTM International, West Conshohocken, PA, USA.
ASTM D-143 (2022). "Standard test methods for small clear specimens of timber," ASTM International, West Conshohocken, PA, USA.
ASTM D245-22 (2022). "Standard practice for establishing structural grades and related allowable properties for visually graded lumber," ASTM International, West Conshohocken, PA, USA.
ASTM E1876-22 (2022). "Standard test method for dynamic Young's modulus, shear modulus, and Poisson's ratio by impulse excitation of vibration," ASTM International, West Conshohocken, PA, USA.
Ballarin, A. W., and Palma, H. A. L. (2003). "Propriedades de resistência e rigidez da madeira juvenil e adulta de *Pinus taeda* L.," *Rev. Árvore* 27(3), 371-380. https://doi.org/10.1590/S0100-67622003000300014
Calil Junior, C., Lahr, F. A. R., and Dias, A. A. (2003). *Dimensionamento de Elementos Estruturais em Madeira*, Manole, Barueri, Brazil.
Candaten, L., Rodrigues, E. F., Trevisan, R., Eloy, E., and Fontoura, M. R. (2018). "Flexão estática e massa específica aparente da madeira de *Inga marginata* em diferentes condições de umidade," *Pesq. Flor. Bras.* 38, 1-5. https://doi.org/10.4336/2018.pfb.38e201801671
Cunha, A. B., and Matos, J. L. M. (2010). "Determinação do módulo de elasticidade em madeira laminada por meio de ensaio não destrutivo ("stress wave timer")," *Rev. Árvore* 34(2), 345-354. https://doi.org/10.1590/S0100-67622010000200018
Dias, A., Gaspar, M. J., Carvalho, A., Pires, J., Lima-Brito, J., Silva, M. E., and Louzada, J. L. (2018). "Within- and between-tree variation of wood density components in *Pinus nigra* at six sites in Portugal," *Ann. For. Sci.* 75, 58. https://doi.org/10.1007/s13595-018-0734-6
Erasmus, J., Kunneke, A., Drew, D. M., and Wessels, C. B. (2018). "The effect of planting spacing on *Pinus patula* stem straightness, microfibril angle and wood density," *Forestry* 91, 247-258. https://doi.org/10.1093/forestry/cpy005
Essien, C., Via, B. K., Cheng, Q., Gallagher, T., McDonald, T., Wang, X., and Eckhardt, L. G. (2017). "Multivariate modeling of acoustomechanical response of 14-year-old suppressed loblolly pine (*Pinus taeda*) to variation in wood chemistry, microfibril angle and density," *Wood Sci Technol* 51, 475-492. https://doi.org/10.1007/s00226-017-0894-9
Fabisiak, E., and Fabisiak, B. (2021). "Relationship of tracheid length, annual ring width, and wood density in Scots Pine (*Pinus sylvestris* L.) trees from different social classes of tree position in the stand," *BioResources* 16(4), 7492. https://doi.org/10.15376/biores.16.4.7492-7508
Ferreira, P. D. S., Ramalho, F. M. G., Couto, A. M., Protásio, T. P., Monteiro, T. C., and Hein, P. R. G. (2023). "Relationship among the stiffness, wave propagation speed, density and moisture content of *Pinus elliottii* and *Bertholletia excelsa* wood specimens," *Wood Mater. Sci. Eng.* 18, 151-160. https://doi.org/10.1080/17480272.2021.1996456
Gonçalez, J. C., Santos, N., Silva Junior, F. D., Souza, R. S., and Paula, M. D. (2018). "Growth ring width of *Pinus caribaea* and its relationship with wood properties," *Sci. For.* 46(120), 670-678. https://doi.org/10.18671/scifor.v46n120.15

Górska, M., Piermattei, A., Ruffinatto, F., and Crivellaro, A. (2025). "Wood mechanical properties scale with distance to tree tip in the outermost growth ring of a Scots pine," *Trees* 39, 31. https://doi.org/10.1007/s00468-025-02608-y

Hébert, F., Krause, C., Plourde, P.Y., Achim, A., Prégent, G., and Ménétrier, J. (2016). "Effect of tree spacing on tree level volume growth, morphology, and wood properties in a 25-year-old *Pinus banksiana* plantation in the boreal forest of Quebec," *Forests* 7(11), article 276. https://doi.org/10.3390/f7110276

Indústria Brasileira de Árvores—IBÁ. *Relatório Anual 2025*: Ano Base 2025. (https://iba.org/wp-content/uploads/2025/10/IBA_relatorio_digital_POR.pdf) accessed 3 March 2026).

ISO 13910 (2005). "Structural timber—Characteristic values of strength-graded timber—Sampling, full-size testing and evaluation," International Organization for Standardization (ISO), Geneva, Switzerland.

Konukcu, A. C., Quin, F., and Zhang, J. (2021). "Effect of growth rings on fracture toughness of wood," *Eur. J. Wood Prod.* 79, 1495-1506. https://doi.org/10.1007/s00107-021-01738-7

Lahr, F. A. R., Chahud, E., Arroyo, F. N., Christoforo, A. L., Rodrigues, E. F. C., Almeida, J. P. B., and Aquino, V. B. M. (2022). "Análise da representatividade e da densidade aparente como estimadoras do módulo de elasticidade da classe C60 da NBR7190:1997," *Ambient. Constr.* 22(1), 139-146. https://doi.org/10.1590/s1678-86212022000100583

Mańkowski, P., Karwat, Z., and Laskowska, A. (2025). "Assessment of the modulus of rupture and modulus of elasticity in static bending of yellow pine earlywood and latewood," *Forests* 16(2), article 265. https://doi.org/10.3390/f16020265

Melo, R. R., Silvestre, R., Oliveira, T. M., and Pedrosa, T. D. (2013). "Variação radial e longitudinal da densidade básica da madeira de *Pinus elliottii* Engelm. com diferentes idades," *Ciênc. Madeira* 4(1), 83-92. https://doi.org/10.12953/2177-6830.v04n01a07

Mensah, P., Pimenta, A. S., Melo, R. R., Amponsah, J., Tuo, G., Chakurah, I., Ampadu, S. D., Buckman, I., Nikoi, M., Minkah, E., Miranda, N. O., and Medeiros, P. L. (2025). "The global supply chain of wood products: A literature review," *Forests* 16(7), article 1036. https://doi.org/10.3390/f16071036

Montgomery, D. C., and Runger, G. C. (2016). *Estatística Aplicada e Probabilidade Para Engenheiros*, 6th Ed., LTC: Rio de Janeiro, Brazil.

Moritani, F. Y., and Calil Junior, C. (2019). "Comparação da resistência ao cisalhamento paralelo às fibras do *Eucalyptus urograndis*: Corpos de prova isentos de defeitos x peças estruturais," in: *Pesquisa Científica e Inovação Tecnológica nas Engenharias*, F. B. M. Tullio (ed.), Atena Editora: Ponta Grossa, Brazil, pp. 133-144.

Mustefaga, E. C., Hillig, E., Tavares, E. L., Sozim, P. C. L., and Rusch, F. (2019). "Caracterização físico-mecânica da madeira juvenil de *Pinus*," *Sci. For.* 47(123), 472-481. https://doi.org/10.18671/scifor.v47n123.09

NBR 7190-2 (2022). "Projeto de Estruturas de Madeira—Parte 2: Métodos de Ensaio Para Classificação Visual e Mecânica de Peças Estruturais de Madeira," Associação Brasileira de Normas Técnicas (ABNT), Rio de Janeiro, Brazil.

Olmedo, G. M., Hornink, B., Arenhardt, B. B., Nunes, A. J., de Oliveira, C., Amaral, I. S., Santos, M. R., Fontana, C., and Oliveira, J. M. (2023). "Growth dynamic and climate signals on abandoned plantation of *Pinus elliottii* in Southern Brazil: A dendrochronological contribution," *Dendrochronologia* 82, article 126136. https://doi.org/10.1016/j.dendro.2023.126136

Pagella, G., Mirra, M., Ravenshorst, G., Gard, W., and Kuilen, J. W. V. (2024). "Characterization of the remaining material and mechanical properties of historic wooden foundation piles in Amsterdam," *Constr. Build. Mater.* 450, article 138616. https://doi.org/10.1016/j.conbuildmat.2024.138616

Paula, M. H., Mesquita, R. R. S., Gonçalez, J. C., Ribeiro, E. S., and Souza, R. S. (2016). "Utilização de métodos não destrutivos para caracterização simplificada da madeira de cumaru (*Dipteryx odorata* Willd)," *Biodiversidade* 15, 136-149.

Pumijumnong, N., Muangsong, C., Buajan, S., Songtrirat, P., Chatwatthana, R., and Chareonwong, U. (2023). "Factors affecting cambial growth periodicity and wood formation in tropical forest trees: a review," *Forests* 14(5), article 1025. https://doi.org/10.3390/f14051025

R Core Team. (2021). *R: A Language and Environment for Statistical Computing*, R Foundation for Statistical Computing, Vienna, Austria.

Rall, R. (2006). *Influência das Características dos Anéis de Crescimento na Densidade, Resistência e Rigidez da Madeira de Pinus taeda L.*, Master's Thesis, Universidade Estadual Paulista, Botucatu, Brazil.

Ruffinatto, F., Negro, F., and Crivellaro, A. (2023). "The macroscopic structure of wood," *Forests* 14(3), article 644. https://doi.org/10.3390/f14030644

Santos, L. L. (2019). *Estabelecimento de Classes de Resistência para a Madeira Serrada de Pinus* spp. Doctoral Thesis, Universidade de São Paulo, São Carlos, Brazil.

Schneider, C. A., Rasband, W. S., and Eliceiri, K. W. (2012). "Image to ImageJ: 25 years of image analysis," *Nat. Methods* 9, 671-675. https://doi.org/10.1038/nmeth.2089

Segundinho, P. G. A., Carreira, M. R., Regazzi, A. J., and Dias, A. A. (2017). "Influência do teor de umidade na determinação do módulo de elasticidade de vigas de *Pinus* sp.," *Ambient. Constr.* 17(3), 319-329. https://doi.org/10.1590/s1678-86212017000300179

Segundinho, P. G. D. A., Regazzi, A. J., Poletti, F. S., Paula, M. O. D., Mendonça, A. R. D., and Gonçalves, F. G. (2018). "Variação dos módulos de elasticidade e ruptura em madeira de cedro-australiano por meio de ensaios não destrutivo e destrutivo," *Ciênc. Florest.* 28(3), 1163-1178. https://doi.org/10.5902/1980509833392

Stöd, R., Marttila, J., Haapala, A., Tomppo, L., and Verkasalo, E. (2025). "Basic density and shrinkage of Scots pine (*Pinus sylvestris* L.) thinning wood," *Eur. J. Wood Wood Prod.* 83(192), article 192. https://doi.org/10.1007/s00107-025-02348-3

Thomte, L., Shah, S. K., Mehrotra, N., Bhagabati, A. K., and Saikia, A. (2022). "Influence of climate on multiple tree-ring parameters of *Pinus kesiya* from Manipur, Northeast India," *Dendrochronologia* 71, article 125906. https://doi.org/10.1016/j.dendro.2021.125906

Topanotti, L. R., Vaz, D. R., Carvalho, S. P. C., Rios, P. D. A., Tomazello-Filho, M., Dobner, M., Jr., and Nicoletti, M. F. (2021). "Growth and wood density of *Pinus taeda* L. as affected by shelterwood harvest in a two-aged stand in Southern Brazil," *Eur. J. Forest Res.* 140, 869-881. https://doi.org/10.1007/s10342-021-01372-1

Trianoski, R., Matos, J. D., Iwakiri, S., and Prata, J. G. (2014). "Avaliação das propriedades mecânicas da madeira de especies de *Pinus* tropicais," *Sci. For.* 42(101), 21-28.

Wang, S., Chen, D., Chu, J., and Jiang, J. (2022). "Effect of growth ring width and latewood content on selected physical and mechanical properties of plantation Japanese larch wood," *Forests* 13(5), article 797. https://doi.org/10.3390/f13050797

Zangiacomo, A. L., Christoforo, A. L., and Lahr, F. A. R. (2013). "Avaliação do módulo de elasticidade de peças estruturais roliças e de corpos-de-prova de *Pinus elliottii*," *Sci. For.* 41(98), 283-291.

Article submitted: April 16, 2026; Peer review completed: May 31, 2026; Revised version received and accepted: June 7, 2026; Published: September 24, 2026.
DOI: 10.15376/biores.21.4.11027-11043